Volume 1 | Number 1 | Jan 2013 | Pages 1–100

Organic & Biomolecular Chemistry

www.rsc.org/obc

ROYAL SOCIETY OF CHEMISTRY

ROYAL SOCIETY OF CHEMISTRY

www.rsc.org/obc

Journal Name

ARTICLE

Oligomycins as inhibitors of K-Ras plasma membrane localisation

A. A. Salim,[a] L. Tan,[b] X.-C. Huang,[a] K.-J. Cho,[b] E. Lacey,[c] J. F. Hancock[b] and R. J. Capon[a]*

Frequently present in pancreatic, colorectal and non-small cell lung carcinomas, oncogenic mutant K-Ras must be localised to the plasma membrane (PM) to be functional. Inhibitors of K-Ras PM localisation are therefore putative cancer chemotherapeutics. By screening a microbial extract library in a high content cell-based assay we detected the rare oligomycin class of *Streptomyces* polyketides as inhibitors of K-Ras PM localisation. Cultivation and fractionation of three unique oligomycin producing *Streptomyces* strains yielded oligomycins A–E (1–5) and 21-hydroxy-oligomycin A (6), together with the new 21-hydroxy-oligomycin C (7) and 40-hydroxy-oligomycin B (8). Structures for 1–8 were assigned by detailed spectroscopic analysis. Cancer cell viability screening confirmed 1–8 were cytotoxic to human colorectal carcinoma cells ($IC_{50} > 3$ μM), and were inhibitors of the ABC transporter efflux pump P-glycoprotein (P-gp), with 5 being comparable in potency to the positive control verapamil. Significantly, oligomycins 1–8 proved to be exceptionally potent inhibitors of K-Ras PM localisation (E_{max} 0.67-0.75 with an $IC_{50} \sim 1.5$–14 nM).

Introduction

Ras proteins are membrane-bound GTPases that regulate cell growth, proliferation and differentiation. Mutant forms of Ras are prominent in many human cancers.[1] For example, of the three ubiquitously expressed mammalian isoforms (H-, N- and K-), constitutively activated mutations of K-Ras are evident in 90% of pancreatic, 45% of colorectal and 35% of non-small cell lung carcinomas.[2] Since oncogenic Ras proteins must be localised to the inner leaflet of the plasma membrane (PM) for biological activity,[3] clinically acceptable inhibitors of K-Ras PM localisation hold great promise as a means to treat K-Ras mutated cancers.[4] Thus, the need to discover new chemical scaffolds capable of mislocalising oncogenic K-Ras remains compelling.

To address this challenge, we examined a library of 500 microbial extracts selected from a library of >300,000 isolates on the basis of their ability to produce secondary metabolites with high chemical diversity. We employed high content quantitative confocal imaging to assess the ability of these extracts to mislocalise oncogenic mutant K-Ras (mGFP-K-Ras G12V) from the PM of intact Madin-Darby canine kidney (MDCK cells).[4a] In proof of concept studies, we documented staurosporine,[4a] oxanthromicins[5] and neoantimycins[6] as promising inhibitors of K-Ras PM localisation. In this report we apply this refined biodiscovery approach to characterise the

nM K-Ras mislocalisation properties of the oligomycins, a rare class of polyketide recovered from a soil-derived *Streptomyces* sp. AS4799 sourced from El Pont de Suert, Spain. As *Streptomyces* sp. AS4799 was a low yield producer of oligomycins, we turned our attention to three superior oligomycin producing strains selected from our (MST) library. *Streptomyces* sp. AS5339v11 sourced from Hay, New South Wales (NSW), Australia, exhibited a co-metabolite profile identical to that of AS4799, while *Streptomyces* sp. AS5958 sourced from Windsor Downs, NSW, and *Streptomyces* sp. AS5351 sourced from Carnarvon, Western Australia, produced unique secondary metabolite profiles - all inclusive of oligomycins. Collectively these three strains yielded six known (1–6) and two new (7–8) oligomycins, along with germicidins A and B (9–10),[7] nemadectins α and γ (11–12)[8] and venturicidin A (13)[9] (Figure 1).

The oligomycins are polyketides featuring a 26-membered macrocyclic lactone fused to a bicyclic spiroketal (1,7-dioxaspiro[5.5]undecanyl) ring system. The oligomycin complex was first reported in 1954 from a strain of *Streptomyces diastatochromogenes*,[10] with a 1958 account resolving this mixture into oligomycins A-C (1–3), albeit without structure elucidation.[11] A 1961 report described antibiotic A272 (rutamycin A), also known as oligomycin D (4), from a strain of *S. rutgersensis,* again without structure elucidation.[12] The structures for 2 and 4 inclusive of relative configurations were subsequently assigned by single-crystal X-ray analysis in 1972[13] and 1978,[14] with absolute configurations confirmed by enantiospecific synthesis in 1993[15] and 1990,[16] respectively. Structures were assigned to 1 and 3 in 1986 based on spectroscopic analysis and correlation of base degradation products with 2,[17] with *ab initio* ^{1}H and ^{13}C NMR assignments reported in 1985 for 1,[18] and in 1998 for 2 and 3,[19] and X-Ray analyses (inclusive of absolute configurations)

[a.] *Institute for Molecular Bioscience, The University of Queensland, St Lucia, QLD 4072, Australia. E-mail: r.capon@uq.edu.au; Fax: +61-7-3346-2090*
[b.] *Integrative Biology and Pharmacology, The University of Texas Medical School, Houston, Texas 77030, USA.*
[c.] *Microbial Screening Technologies Pty. Ltd., Building C 28-54 Percival Road, Smithfield, NSW 2164, Australia.*

Organic & Biomolecular Chemistry Accepted Manuscript

reported for **2** in 2008[20] and **3** in 2010.[21] Oligomycin E (**5**) was reported in 1987 from *Streptomyces* sp. MCI-2225, and its structure and relative configuration were assigned by NMR analysis.[22] A single-crystal X-ray analysis in 2007 established the structure and absolute configuration of 21-hydroxy-oligomycin A (**6**) isolated from *Streptomyces cyaneogriseus* ssp. *noncyanogenus*.[23] The structures for several other oligomycins described in the scientific and/or patent literature are largely limited to planar structures. Oligomycins have been attributed antifungal,[11] antitumour,[22, 24] immunosuppresive,[25] and insecticidal and nematocidal[26] properties, and have been noted as inhibitors of mitochondrial F_0F_1-ATPase[27] and the ABC transporter multidrug resistance efflux pump P-glycoprotein (P-gp).[28]

Results and discussion

Bioassay-guided fractionation of cultivations of our three prioritised *Streptomyces* strains yielded three distinct polyketide profiles, dominated by macrolactones. *Streptomyces* sp. AS5339v11 yielded oligomycins A–C (**1–3**) and E (**5**), germicidins A and B (**9–10**),[7] and low yields of the new 40-hydroxy-oligomycin B (**8**). *Streptomyces* sp. AS5351 yielded 21-hydroxy-oligomycin A (**6**), nemadectin α and γ (**11–12**),[8] and the new 21-hydroxy-oligomycin C (**7**). *Streptomyces* sp. AS5958 yielded oligomycin D (**4**) and venturicidin A (**13**).[9] The structures for the known oligomycins **1–6** and the co-metabolites **9–13** were confirmed by detailed spectroscopic analysis. An account of the structure elucidation of the new oligomycins **7–8**, and an assessment of the cytotoxicity and P-gp/K-Ras inhibitory properties of **1–8**, is detailed below.

HRESI(+)MS measurements returned a molecular formula for **7** ($C_{45}H_{74}O_{11}$, Δppm – 0.3) suggestive of a deoxy analogue of the co-metabolite 21-hydroxy-oligomycin A (**6**). Diagnostic 2D NMR (DMSO-d_6) correlations for **7** established a planar structure where the principle difference with **6** was the absence of the 12-OH moiety (Figure 2). This structural relationship was further evidenced in the 1D NMR data (ESI Table S1) where the C-12 tertiary alcohol and pendant tertiary methyl evident in **6** ($δ_H$ 0.92, s, H$_3$-39; $δ_C$ 22.0, C-39; 82.6, C-12), was replaced by a secondary methyl in **7** ($δ_H$ 0.74, d, 6.8 Hz, H$_3$-39; $δ_C$ 13.3, C-39; 49.4, C-12). Excellent concordance in NMR data (particularly ROESY correlations, ESI Figure S9) between **7** and **6** permitted assignment of the structure (relative configuration) and trivial nomenclature for 21-hydroxy-oligomycin C (**7**), while comparable specific rotations between **7** (−37.2) and **6** (−39.6), and their occurrence as biosynthetically related co-metabolites in *Streptomyces* AS5351, was supportive of a common absolute configuration.

HRESI(+)MS analysis of **8** returned a molecular formula ($C_{45}H_{72}O_{13}$, Δppm – 1.8) isomeric with the *Streptomyces* AS5339v11 co-metabolite oligomycin E (**5**). Diagnostic 2D NMR (DMSO-d_6) correlations established a planar structure in which the 26-OH in **5** had been replaced by a 40-OH in **8** (Figure 2). This structural relationship was further evidenced in the 1D NMR data (Table S2) with the C-14 secondary methyl ($δ_H$ 0.99,

d, 6.8 Hz, H$_3$-40; $δ_C$ 33.3, C-14; 14.9, C-40) and C-26 tertiary alcohol ($δ_H$ 4.11, OH-26; 1.13, s, H$_3$-44; $δ_C$ 72.7, C-26; 21.0, C-44) in **5** being replaced by a C-14 hydroxymethylene ($δ_H$ 3.27/3.67, H$_2$-40; $δ_C$ 40.6, C-14; 60.3, C-40) and a C-26 tertiary methine ($δ_H$ 2.36, m, H-26; 0.75, d, 6.6 Hz, H$_3$-44; $δ_C$ 30.9, C-26; 11.5, C-44) in **8**. Excellent concordance in the NMR data (particularly ROESY correlations, Figure S10) between **8** and **5** permitted assignment of the structure (relative configuration) and trivial nomenclature for 40-hydroxy-oligomycin B (**8**), while comparable specific rotations between **8** (−27.9) and **5** (−32.8), and their occurrence as biosynthetically related co-metabolites in *Streptomyces* AS5339v11, was supportive of a common absolute configuration.

(**1**) R$_1$ = OH R$_2$ = H R$_3$ = CH$_3$
(**3**) R$_1$ = H   R$_2$ = H R$_3$ = CH$_3$
(**4**) R$_1$ = OH R$_2$ = H R$_3$ = H
(**6**) R$_1$ = OH R$_2$ = OH R$_3$ = CH$_3$
(**7**) R$_1$ = H   R$_2$ = OH R$_3$ = CH$_3$

(**2**) R$_1$ = H   R$_2$ = H
(**5**) R$_1$ = H   R$_2$ = OH
(**8**) R$_1$ = OH R$_2$ = H

(**9**) R = CH$_3$
(**10**) R = H

(**11**) R$_1$ = i-Pr, R$_2$ = H
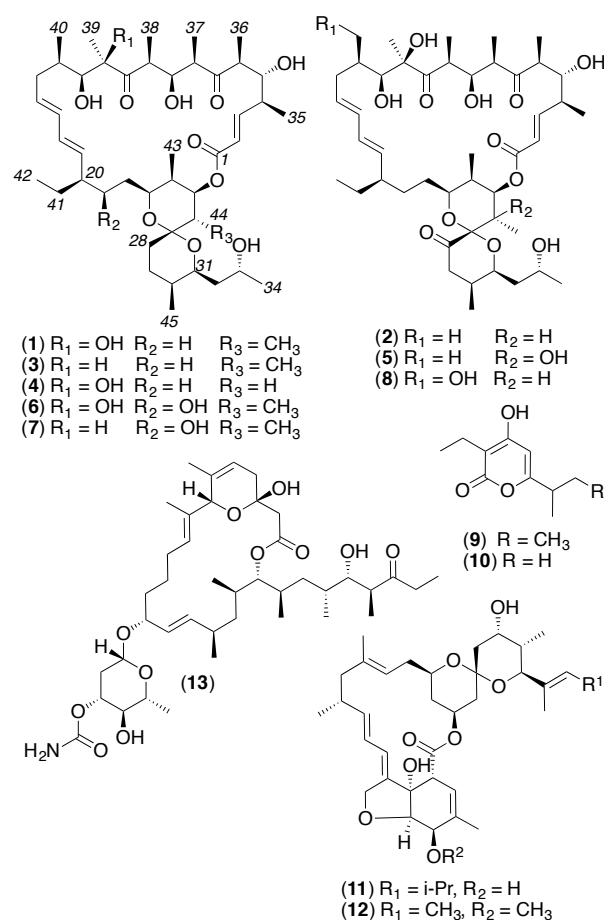(**12**) R$_1$ = CH$_3$, R$_2$ = CH$_3$

Fig 1. *Streptomyces* metabolites **1 - 13**
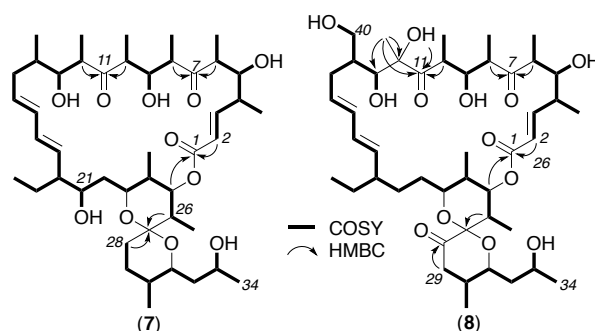

— COSY
⌒ HMBC

Fig 2. Diagnostic 2D NMR corelations for **7** and **8**

We employed quantitative confocal imaging to measure the ability of **1–8** to mislocalise oncogenic mutant K-Ras (mGFP-K-Ras G12V) from the PM of MDCK cells, using an optimized high content assay methodology.[4a] MDCK cells stably expressing mGFP-KRasG12V and mCherry-CAAX (an endomembrane marker) were treated with oligomycins for 48 h, and cells were fixed with 4% PFA and imaged by a confocal microscope. K-Ras mislocalisation from the plasma membranes were calculated using Manders coefficients (E), by measuring the fraction of mCherry-CAAX co-localising with mGFP-K-RasG12V (maximum co-localisation gives a value of E=1). Manders coefficients values were evaluated at different oligomycin concentrations. The dose response curve was fitted with a four-parameter non-linear regression curve and IC_{50} values derived using Prism statistic software (ver5.0c). The E_{max} value from the same fit reflects the maximum extent of mislocalisation of K-Ras from the plasma membrane to endomembrane. These experiments established, as predicted from primary screening data, that the oligomycins **1–8** were potent (low nM) inhibitors of K-Ras (Table 1), but have minimal effect on H-Ras PM localisation (Figure 3).

Table 1 Assessment of **1-8** as inhibitors of K-Ras PM localisation in MDCK cell

	E_{max}[a]	IC_{50} (nM)[b]
1	0.75 ± 0.02	1.44 ± 0.03
2	0.67 ± 0.02	3.51 ± 0.16
3	0.72 ± 0.03	7.25 ± 0.14
4	0.72 ± 0.01	3.49 ± 0.08
5	0.73 ± 0.06	4.90 ± 0.64
6	0.76 ± 0.04	4.82 ± 0.70
7	0.68 ± 0.01	14.1 ± 0.24
8	0.73 ± 0.05	5.91 ± 1.62

[a]E_{max} = Highest Manders coefficient which describe the maximum extent of K-Ras PM mislocalisation. [b]IC_{50} = Concentration needed for 50% PM mislocalisation.
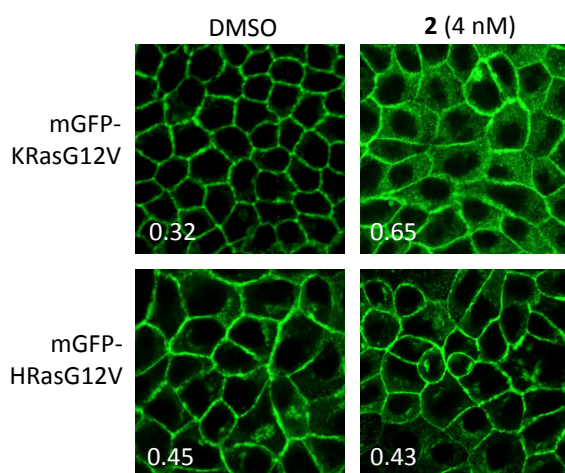

Fig 3. MDCK cells stably co-expressing mCherry-CAAX and mGFP-KRasG12V or –HRasG12V were treated with 4 nM oligomycin B (**2**) for 48h. Insert: Manders coefficients for the representative images.

In 2001, oligomycin A (**1**) was described as among the top 0.1% most cell line selective cytotoxic agent from 37,000 molecules tested against the National Cancer Institute (NCI)

panel of 60 human cancer cell lines, with ~35% of cell lines exquisitely sensitive (GI_{50} 10 nM) and the remaining less insensitive (GI_{50} 1-10 µM).[29] More recent NCI online data (http://dtp.nci.nih.gov) reveals comparable levels of selective cytotoxicity for **2** and **3** against the same panel of cancer cell lines. In 2004 an (unspecified) oligomycin was described as an inhibitor of the multidrug resistance efflux pump P-glycoprotein (P-gp).[28] To the best of our knowledge there have been no accounts on the P-gp inhibitory properties of specific oligomycins.

As up-regulation of P-gp in cancers can lead to accelerated drug efflux from cells, it is important to assess potential drug candidates for susceptibility to P-gp mediated efflux. To investigate the susceptibility of **1–8** we employed a resazurin cell viability assay to quantify cytotoxicity against the colon cancer cell line SW620, and its P-gp over-expressing daughter cell line SW620 Ad300. To validate our approach, we first confirmed that SW620 Ad300 cells were 22-fold less sensitive (FR = 22) to doxorubicin (adriamycin) than the parent SW620 cells, and that co-administration of the positive control P-gp inhibitor verapamil increased the sensitivity of the SW620 Ad300 cells to doxorubicin (FR = 2.4). Armed with a validated assay we determined that **1–8** were moderately cytotoxic towards both SW620 and SW620 Ad300 cells (IC_{50} >3 µM), and were not subject to P-gp mediated efflux (FR = 0.27-1.2) (Table 2).

Table 2 Assessment of **1-8** for cytotoxicity and susceptibility to P-gp mediated efflux

	SW620 IC_{50} (µM)	SW620 Ad300 IC_{50} (µM)	FR[a]
1	14.6 ± 2.5	4.0 ± 1.1	0.27
2	17.0 ± 0.6	12.9 ± 1.3	0.76
3	19.8 ± 1.2	22.5 ± 3.8	1.1
4	36.0 ± 2.3	12.9 ± 1.0	0.35
5	7.1 ± 0.4	4.0 ± 0.8	0.56
6	14.4 ± 0.6	11.8 ± 3.1	0.82
7	5.7 ± 0.9	3.1 ± 0.2	0.54
8	13.6 ± 0.4	16.4 ± 1.5	1.2

[a]FR = fold resistance, calculated as the ratio IC_{50} SW620Ad300 / IC_{50} SW620.

To further investigate the relationship between **1–8** and P-gp we employed a calcein AM flow cytometry assay, using a methodology optimized and documented during earlier studies.[30] Briefly, the non-fluorescent reagent calcein AM is both a P-gp substrate and undergoes intracellular hydrolysis by esterases to yield the fluorescent dye calcein. Functioning P-gp mediates efflux of calcein AM prior to hydrolysis, resulting in reduced levels of intracellular fluorescence. In the presence of a P-gp inhibitor, calcein AM efflux is blocked, resulting in higher levels of intracellular fluorescence. In the flow cytometry assay, **1–8** (20 µM) increased intracellular calcein fluorescence significantly compared to the negative control (Figure 4) (fluorescence arbitrary ratios (FAR) = 15-48). In these studies, **5** is the most potent P-gp inhibitor (FAR = 48.2), comparable to the positive control verapamil (FAR = 41.3).
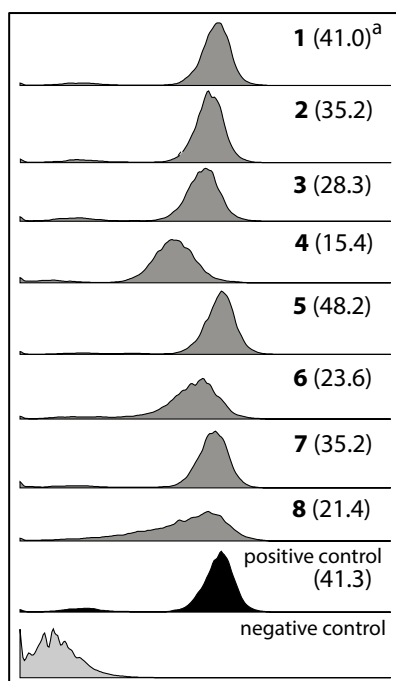
Fig 4. The effect of oligomycins on the accumulation of calcein AM in P-gp over-expressing SW620 Ad300 cells analysed using flow cytometry. [a]FAR (fluorescence arbitrary ratio) = calcein fluorescence intensity (geometric mean) in the presence of **1**–**8** (20 μM) / phosphate buffer saline (negative control). Positive and negative controls are verapamil (20 μM) and PBS, respectively.

Conclusions

This current study validates microbial biodiscovery supported by high content quantitative confocal imaging as an effective means to discover new inhibitors of oncogenic K-Ras PM localisation. By applying this strategy we successfully detected, sourced, isolated, characterised and identified six known (**1**–**6**) and two new (**7**–**8**) oligomycins, along with the co-metabolites **9**–**13**, from three diverse soil-derived *Streptomyces* strains, and established **1**–**8** as μM inhibitors of the multidrug efflux pump P-gp, and low nM inhibitors of K-Ras PM localisation. Ongoing investigations into the K-Ras inhibitory mechanism of action of **1**–**8** are expected to reveal pathways and molecular targets critical to controlling K-Ras. Our investigations into the K-Ras PM mislocalisation mechanism–of–action of **1**-**8** are nearing completion, and will be published elsewhere. Knowledge of the inhibitor properties of oligomycins **1**-**8** on K-Ras could inform the development of new probes to better interrogate, and new therapeutics to better treat, K-Ras dependent cancers.

Experimental section

Characterisation of compounds

oligomycin A (1). Colourless amorphous solid; $[\alpha]_D^{22}$ –47.3 (*c* = 0.083, MeOH); ^{1}H & ^{13}C NMR (DMSO-d_6) see Tables S3a and 4, and Figures S1a and S1b; HRESI(+)MS *m/z* 813.5126 [M+Na]$^+$ (calcd for $C_{45}H_{74}O_{11}Na$, 813.5123).

oligomycin B (2). Colourless amorphous solid; $[\alpha]_D^{22}$ –67.0 (*c* = 0.115, MeOH); ^{1}H & ^{13}C NMR (DMSO-d_6) see Tables S3a and 4, and Figures S2a and S2b; HRESI(+)MS *m/z* 827.4909 [M+Na]$^+$ (calcd for $C_{45}H_{72}O_{12}Na$, 827.4916).

oligomycin C (3). Colourless amorphous solid; $[\alpha]_D^{22}$ –36.8 (*c* = 0.15, MeOH); ^{1}H & ^{13}C NMR (DMSO-d_6) see Tables S3b and 4, and Figures S3a and S3b; HRESI(+)MS *m/z* 797.5181 [M+Na]$^+$ (calcd for $C_{45}H_{74}O_{10}Na$, 797.5174).

oligomycin D (4). Colourless amorphous solid; $[\alpha]_D^{22}$ –29.5 (*c* = 0.075, MeOH); ^{1}H & ^{13}C NMR (DMSO-d_6) see Tables S3b and 4, and Figures S4a and S4b; HRESI(+)MS *m/z* 799.4968 [M+Na]$^+$ (calcd for $C_{44}H_{72}O_{11}Na$, 799.4967).

oligomycin E (5). Colourless amorphous solid; $[\alpha]_D^{22}$ –32.8 (*c* = 0.13, MeOH); ^{1}H & ^{13}C NMR (DMSO-d_6) see Tables S3b and 4, and Figures S5a and S5b; HRESI(+)MS *m/z* 843.4853 [M+Na]$^+$ (calcd for $C_{45}H_{72}O_{13}Na$, 843.4865).

21-hydroxy-oligomycin A (6). Colourless amorphous solid; $[\alpha]_D^{22}$ –39.6 (*c* = 0.24, MeOH); ^{1}H & ^{13}C NMR (DMSO-d_6) see Tables S3a and 4, and Figures S6a and S6b; HRESI(+)MS *m/z* 829.5067 [M+Na]$^+$ (calcd for $C_{45}H_{74}O_{12}Na$, 829.5072).

21-hydroxy-oligomycin C (7). Colourless amorphous solid; $[\alpha]_D^{22}$ –37.2 (*c* = 0.105, MeOH); NMR (DMSO-d_6) see Table S1, and Figures S7a and S7b; HRESI(+)MS *m/z* 813.5120 [M+Na]$^+$ (calcd for $C_{45}H_{74}O_{11}Na$, 813.5123).

40-hydroxy-oligomycin B (8). Colourless amorphous solid; $[\alpha]_D^{22}$ –27.9 (*c* = 0.14, MeOH); NMR (DMSO-d_6) see Table S2, and Figures S8a and S8b; HRESI(+)MS *m/z* 843.4847 [M+Na]$^+$ (calcd for $C_{45}H_{72}O_{13}Na$, 843.4865).

germicidin A (9). Yellow amorphous solid. NMR (CDCl$_3$) see Figures S12; HRESI(+)MS *m/z* 219.0991 [M+Na]$^+$ (calcd for $C_{11}H_{16}O_3Na$, 219.0992).

germicidin B (10). Yellow amorphous solid. NMR (CDCl$_3$) see Figures S13; HRESI(+)MS *m/z* 205.0831 [M+Na]$^+$ (calcd for $C_{10}H_{14}O_3Na$, 205.0835).

nemadectin α (11). White amorphous solid. NMR (CDCl$_3$) see Figures S14; HRESI(+)MS *m/z* 635.3538 [M+Na]$^+$ (calcd for $C_{36}H_{52}O_8Na$, 635.3554).

nemadectin γ (12). White amorphous solid. NMR (CDCl$_3$) see Figures S15; HRESI(+)MS *m/z* 621.3416 [M+Na]$^+$ (calcd for $C_{35}H_{50}O_8Na$, 621.3398).

venturicidin A (13). Colourless amorphous solid. NMR (CDCl$_3$) see Figures S16; HRESI(+)MS *m/z* 772.4607 [M+Na]$^+$ (calcd for $C_{41}H_{67}O_{11}Na$, 772.4606).

Acknowledgements

Organic & Biomolecular Chemistry Accepted Manuscript

Notes and references

1   J. F. Hancock, *Nat. Rev. Mol. Cell Biol.* 2003, **4**, 373-385.
2   B. O. Bodemann and M. A. White, *Curr. Biol.* 2013, **23**, R17-R20.
3   A. T. Baines, D. Xu and C. J. Der, *Future Med. Chem.* 2011, **3**, 1787-1808.
4   (a) K.-j. Cho, J.-H. Park, A. M. Piggott, A. A. Salim, A. A. Gorfe, R. G. Parton, R. J. Capon, E. Lacey and J. F. Hancock, *J. Biol. Chem.* 2012, **287**, 43573-43584; (b) D. van der Hoeven, K.-j. Cho, X. Ma, S. Chigurupati, R. G. Parton and J. F. Hancock, *Mol. Cell. Biol.* 2013, **33**, 237-251.
5   A. A. Salim, X. Xiao, K.-J. Cho, A. M. Piggott, E. Lacey, J. F. Hancock and R. J. Capon, *Org. Biomol. Chem.* 2014, **12**, 4872-4878.
6   A. A. Salim, K.-J. Cho, L. Tan, M. Quezada, E. Lacey, J. F. Hancock and R. J. Capon, *Org. Lett.* 2014, **16**, 5036-5039.
7   F. Petersen, H. Zaehner, J. W. Metzger, S. Freund and R. P. Hummel, *J. Antibiot.* 1993, **46**, 1126-1138.
8   (a) G. T. Carter, J. A. Nietsche and D. B. Borders, *J. Chem. Soc., Chem. Commun.* 1987, 402-404; (b) L. C. Lo, N. Berova, K. Nakanishi, G. Schlingmann, G. T. Carter and D. B. Borders, *J. Am. Chem. Soc.* 1992, **114**, 7371-7374.
9   (a) M. Brufani, L. Cellai, C. Musu and W. Keller-Schierlein, *Helv. Chim. Acta* 1972, **55**, 2329-2346; (b) A. Rhodes, K. H. Fantes, B. Boothroyd, M. P. McGonagle and R. Crosse, *Nature* 1961, **192**, 952-954.
10 R. M. Smith, W. H. Peterson and E. McCoy, *Antibiot. Chemother.* 1954, **4**, 962-970.
11 S. Masamune, J. M. Sehgal, E. E. Van Tamelen, F. M. Strong and W. H. Peterson, *J. Am. Chem. Soc.* 1958, **80**, 6092-6095.
12 (a) R. Q. Thompson, M. M. Hoehn and C. E. Higgens, *Antimicrob. Agents Chemother.* 1961, 474-480; (b) P. D. Shaw in *Antibiotics*, *Vol. 1*, Eds. D. Gottlieb and P. D. Shaw, Springer-Verlag, Berlin, **1967**, pp. 585-610.
13 M. Von Glehn, R. Norrestam, P. Kierkegaard, L. Maron and L. Ernster, *FEBS Lett.* 1972, **20**, 267-269.
14 B. Arnoux, M. C. Garcia-Alvarez, C. Marazano, B. C. Das, C. Pascard, C. Merienne and T. Staron, *J. Chem. Soc., Chem. Commun.* 1978, 318-319.
15 M. Nakata, T. Ishiyama, Y. Hirose, H. Maruoka and K. Tatsuta, *Tetrahedron Lett.* 1993, **34**, 8439-8442.
16 D. A. Evans, D. L. Rieger, T. K. Jones and S. W. Kaldor, *J. Org. Chem.* 1990, **55**, 6260-6268.
17 G. T. Carter, *J. Org. Chem.* 1986, **51**, 4264-4271.
18 G. A. Morris and M. S. Richards, *Magn. Reson. Chem.* 1985, **23**, 676-683.
19 L. Szilagyi and K. Feher, *J. Mol. Struct.* 1998, **471**, 195-207.
20 R. A. Palmer and B. S. Potter, *J. Chem. Crystallogr.* 2008, **38**, 243-253.
21 P. W. Yang, M. G. Li, J. Y. Zhao, M. Z. Zhu, H. Shang, J. R. Li, X. L. Cui, R. Huang and M. L. Wen, *Folia Microbiol.* 2010, **55**, 10-16.
22 K. Kobayashi, C. Nishino, J. Ohya, S. Sato, T. Mikawa, Y. Shiobara, M. Kodama and N. Nishimoto, *J. Antibiot.* 1987, **40**, 1053-1057.
23 M. M. Wagenaar, R. T. Williamson, D. M. Ho and G. T. Carter, *J. Nat. Prod.* 2007, **70**, 367-371.
24 M. Yamazaki, T. Yamashita, T. Harada, T. Nishikiori, S. Saito, N. Shimada and A. Fujii, *J. Antibiot.* 1992, **45**, 171-179.
25 H. Laatsch, M. Kellner, G. Wolf, Y. S. Lee, F. Hansske, S. Konetschny-Rapp, U. Pessara, W. Scheuer and H. Stockinger, *J. Antibiot.* 1993, **46**, 1334-1341.
26 Y. Enomoto, K. Shiomi, A. Matsumoto, Y. Takahashi, Y. Iwai, A. Harder, H. Kolbl, H. B. Woodruff and S. Omura, *J. Antibiot.* 2001, **54**, 308-313.
27 (a) H. S. Penefsky, *Proc. Natl. Acad. Sci. U. S. A.* 1985, **82**, 1589-1593; (b) J. Symersky, D. Osowski, D. E. Walters and M. Mueller David, *Proc Natl Acad Sci U S A* 2012, **109**, 13961-13965.
28 Y. C. Li, K. P. Fung, T. T. Kwok, C. Y. Lee, Y. K. Suen and S. K. Kong, *Chemotherapy* 2004, **50**, 55-62.
29 A. R. Salomon, D. W. Voehringer, L. A. Herzenberg and C. Khosla, *Chem. Biol.* 2001, **8**, 71-80.
30 (a) X.-c. Huang, Y.-L. Sun, A. A. Salim, Z.-S. Chen and R. J. Capon, *Biochem. Pharmacol.* 2013, **85**, 1257-1268; (b) C. J. Henrich, H. R. Bokesch, M. Dean, S. E. Bates, R. W. Robey, E. I. Goncharova, J. A. Wilson and J. B. McMahon, *J. Biomol. Screening* 2006, **11**, 176-183.